THE SNAPSHOT OF NANOSECOND DEVELOPMENT OF HIGH POWER MICROWAVE VACUUM WINDOW BREAKDOWN

C. CHANG[1,2,*], M. ZHU[1], C. H. CHEN[1,*], M. N. GUO[1], J. C. PENG[1], S. LI[1], Z. F. XIONG[1,2]

[1]Science and Technology on High power microwave Laboratory, NINT, 710024, Xi'an City, China
[2]Department of Engineering Physics, Tsinghua University, Beijing 100084, China
*chang@slac.stanford.edu

ABSTRACT

Breakdown at the vacuum/dielectric interface is triggered by multipactor and finally realized by plasma avalanche in the ambient desorbed or evaporated gas layer above the dielectric. We have theoretically and experimentally demonstrated that the periodic surface profiles and external resonant magnetic field can prominently increase the high power microwave (HPM) breakdown thresholds.

The recent experiments of diagnosing the snapshot of nanosecond development of vacuum window breakdown are reported in this paper. For a flat-surface window, the light emission from the local plasma is focused in a thin layer above the surface during the HPM pulse, and the light emission lasts much longer than the HPM pulse, the thickness increases and the light weakens. The periodic surface could effectively suppress multipactor demonstrated by a much weaker light emission compared with flat surface.

1. INTRODUCTION

The transmission and radiation sub-system in high power microwave (HPM) system emits microwave into atmosphere by antennas. The dielectric window is applied to isolate the air and vacuum. While, the dielectric window breakdown at the vacuum side is the major factor of limiting the maximum radiation power of HPM, which is the bottleneck and challenge in the development of HPM [1].

HPM breakdown at the vacuum/dielectric interface is the result of a series of complex physical processes, which is firstly triggered by secondary electron multipactor and finally realized by plasma avalanche in the ambient desorbed or evaporated gas layer above the dielectric. The initial seed electrons are guided by HPM field and strike on the dielectric surface to yield secondary electrons. Secondary electron multipactoring occurs once SEY is bigger than 1, and then the number of electron dramatically increases till it is saturated [2]. Neuber et al. [3] detected spectral emissions from hydrogen atoms and carbon ions in the HPM window breakdown experiments, proving that the final breakdown occurs in the desorbed or evaporated gas cloud. They observed the cessation of the x-ray radiation generated by bremsstrahlung of impacting electrons after the discharge arc occurred. This demonstrated that a local high pressure was formed above the dielectric, resulting in a significant decrease of electron energy.

Suppressing HPM vacuum multipactor and improving the breakdown thresholds by periodic surface profiles have been theoretically and proof-of-principle experimentally researched [4, 5]. The suppression mechanisms were analyzed by dynamic calculation and simulation. The basic principle of suppression is to alternate the trajectories, flight time and the impact energy of the electrons. The periodic surface can effectively decrease the impact energy to be lower than the first crossover energy of the secondary emission yield, and diminish the flight time of electrons to be much smaller than half of the rf period, leading to the secondary yield smaller than one and multipactor can be quickly and stably restrained.

By using an external dc magnetic field $\boldsymbol{B}\perp(\boldsymbol{E}_{rf}\times\boldsymbol{k})$, where $\boldsymbol{k}$ points to the wave propagation direction, satisfying the gyro-frequency close to the rf frequency $\Omega\sim\omega$ [6, 7], multipactor electrons emitted from the vacuum surface can be resonantly accelerated under $\boldsymbol{E}_{rf}\times\boldsymbol{B}$ to increase the impact energy ε_e by a factor of 5-10 compared with $e^2E_0^2/(2m\omega^2)$, leading to ε_e higher than the second crossover energy ε_{p2} and SEY<1. More importantly, the

corresponding flight time τ~T is independent of the amplitude of $\boldsymbol{E}_{rf}$ and is also the period of the vector $\boldsymbol{E}_{rf}\times\boldsymbol{B}$. Electrons undergo two reverses of the vector during flight, and the phase of $\boldsymbol{E}_{rf}$ for electrons impacting the surface is basically the same with that for electrons emitting from the surface. Thus, secondary electrons undergo $\boldsymbol{E}_{rf}$ in the same direction, and directionally drift under $\boldsymbol{E}_{rf}\times\boldsymbol{B}$, resulting in a stable and rapid multipactor suppression [8].

Although the methods of periodic surface profiles and resonant magnetic field have been demonstrated to effectively suppress multipactor, the underlying breakdown mechanism is still not quite clear, and the way to completely restrain multipactor is needed to go. Besides, Neuber et al. [3] mainly conducted the microwave window vacuum breakdown experiments at microsecond pulse. The main physical factors of breakdown between their microsecond pulse and the nanosecond pulse in our case are quite different, since the recombination and attachment courses are less important during the nanosecond HPM pulse, and higher ionization rate arose from the stronger E-field are needed to realize the ultra fast discharge. Moreover, the space charge field might be an important factor on the rapid breakdown.

2. EXPERIMENTS

In our experiment, the time-dependent and spatial-developing optical emissions of high-power microwave discharge near the dielectric/vacuum interface under nanosecond pulse width and giga-watt power have been observed by the nanosecond-response four-framing ICCD cameras. The four-frame high-speed ICCD illustrated in Fig.1 is consisted of four parts: optical lenses, optical frame system, fast-trigger system (including image intensifier, synchronization machine, time delay device, fast-gate pulse circuit, high voltage power source), and image collecting and processing system.

The working principle of the four-frame ICCD is the following, by the external high-power microwave signal triggering the synchronization machine of the fast-gate system. The synchronization machine exports multi-signals, and the four signals after the time delay device respectively trigger the fast-gate generator, and the other one triggers the image collector. The object is divided to four ways by the optical frame system, each signal couples to the corresponding intensifier, and the picture on the screen of the intensifier. The trigger and collecting data of ICCD is illustrated in Fig.2.

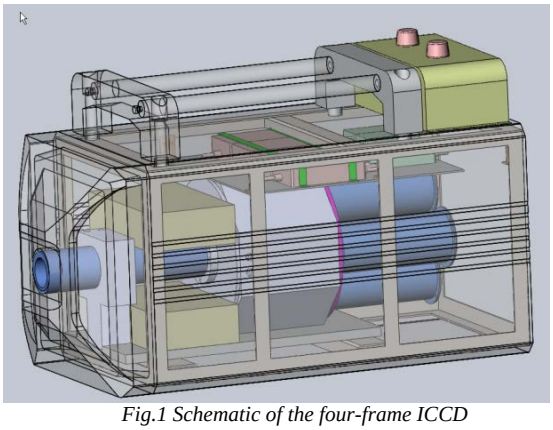

Fig.1 Schematic of the four-frame ICCD

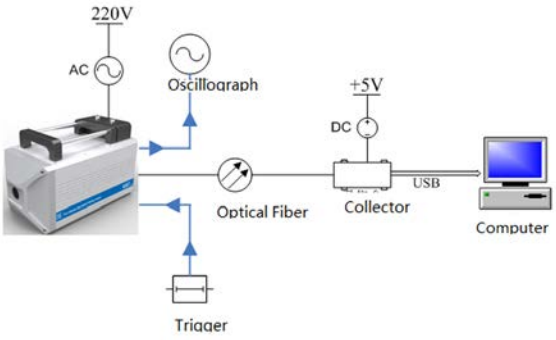

Fig.2 Schematic of the trigger and collecting data of ICCD

The HPM experiment was carried out. The 9.9GHz backward wave oscillator (BWO) produces 1GW of output power in 15ns pulses. The TM01 mode generated in BWO is converted to TE11 mode by the mode convertor, and then radiated to air through a large flare-angle conical horn with 30^{o}. The dielectric windows have the integral multiple of the half guided wavelength to realize the minimum reflection, periodic patterned surface has been used to improve the vacuum breakdown threshold [8], and windows made by polyethylene (PE) as well as polystyrene (PS) material are studied. The high E-field region is focused at the center of the dielectric window with an aperture of 300mm, and nylon bolts were used to fix the window on the horn, preventing from the triple junctions. The intensity of visible light emission as a function of the time and space was measured by a high speed intensified-charged-coupled device (ICCD) camera with four frames. The system trigger delay time of ICCD is as short as 13ns, and its gate width could be selected as 2ns, 5ns, and 10ns; the delay time between two frames could be chosen as 5ns. The time

synchronization between the ICCD and nanosecond microwave pulses is very important, which is realized by using the monitored voltage signal (+65V) from the high-voltage vacuum diode to trigger the fast gate of ICCD. The lenses center of the ICCD camera was located at the horn aperture and placed perpendicular to the HPM propagation to laterally observe the light emission.

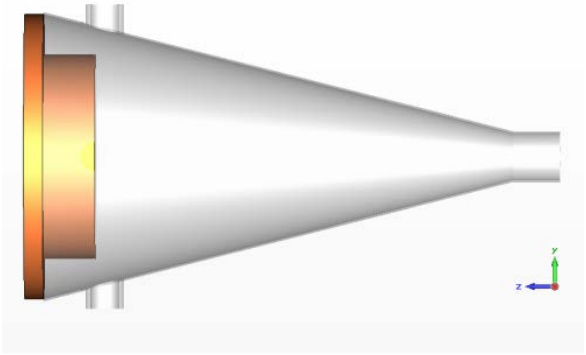

Fig. 3 The model of the horn with punctured holes at side-view

The online and the far-field HPM waveform are also detected. Directional couplers, attenuators, coaxial transmission lines, and crystal diode detectors were used as the sub-systems for online and far-field measurement. The output voltage is monitored by Agilent Infiniium DSO8104A.

The HPM horn used in the diagnostic is shown in Fig.3. The side of the HPM horn is punctured to observe the optical emission at the dielectric surface.

3. EXPERIMENTAL RESULTS AND ANALYSIS

For a flat-surface window, at initial stage, when the microwave starts, there is no light observed. The typical imageof the visible light of HPM breakdown measured by the ICCD is shown in Fig.4.

Initially, before the HPM arrives at the window, there is no light observed. After 5ns, the light emission is concentrated in a 2mm ambient layer above the dielectric surface. The light intensity and emission area increases during the flat top and trailing edge of HPM pulse. The light emission layer becomes thicker to sub-centimeter and gets brighter after the HPM pulse, and then the intensity quickly delays before the whole area becomes completely dark,. From the above analysis, it is indicated that the plasma discharge at the dielectric/vacuum interface under the nanosecond HPM pulse, initially starts at the ambient layer above the surface; the high intense light emission in the surface layer has a thickness of several millimeters and could become brighter after the HPM pulse.

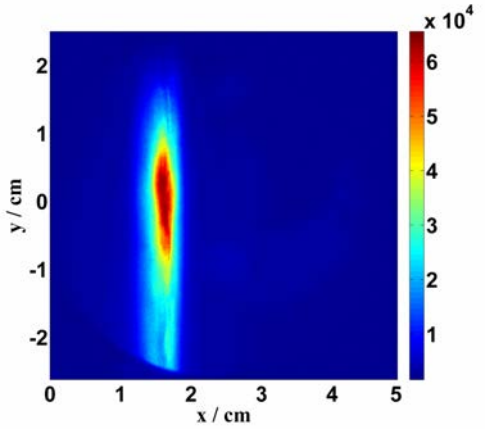

Fig.4 The typical image of visible light in front of the dielectric surface

The mechanism of plasma discharge is explained in the following. Since HPM driven breakdown at the vacuum/dielectric interface is triggered by secondary electron multipactor and finally realized by plasma avalanche in the ambient desorbed or evaporated gas layer above the dielectric [5-8]. When the plasma frequency ω_p reaches the RF frequency ω, i.e., the critical density n_c satisfies $\omega_p^2 = n_c e^2 / (\varepsilon_0 m) = \omega^2$, the microwave transmission cuts off. In order to reach $n_c \sim 1.11*10^{13}/\lambda^2 cm^{-3}$ in a nano-second short HPM pulse, the ambient desorbed or evaporated gas pressure above the dielectric window should be sufficiently high to realize the ultra fast ionization. Thus, what is the estimated local pressure?

The plasma density exponentially increases during the ionization avalanche in the short pulse, i.e. $n_c = n_{e0} \exp\left(\int_0^\tau \nu_i dt\right)$, where n_{e0} is the initial pressure, τ is the pulse width, and ν_i is the ionization rate. Assuming that the surface pressure rising linearly with time t, i.e. $p=(at+p_0)$, where p_0 is the initial pressure and a is the slope coefficient, the ionization frequency can be described as $\nu_i=\nu_i/p*(at+p_0)$. The ratio value of $\nu_i/p \sim 5*10^9/(s*Torr)$ approximately keeps constant for electron energy with several hundreds of eV. [8] Thus, $\ln(n_c/n_{e0})-\nu_i/p*(a\tau^2/2+p_0\tau)=0$. Set $n_c/n_0 \sim 10^{8-10}$, $p_0=10^{-4}$ Torr, and τ=10-20ns, the local pressure need rises to 0.4–0.9 Torr in order to realize ultra fast HPM breakdown. In fact, the ambient pressure was demonstrated to reach 1 Torr in the short-pulse HPM breakdown experiments [8]. The local high pressure above the dielectric surface,

in a layer thickness of sub-centimeter, may come from the desorption gas induced by multipactor electrons, and intense ionization mainly occurs in this layer.

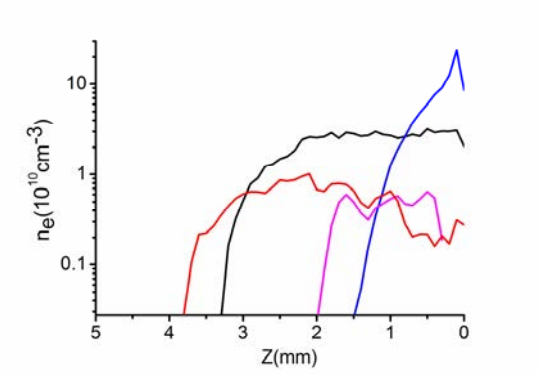

Fig.5 Variation of plasma-electron density ne with space Z; (Red, Black, Blue, and Pink curves in sequence).

Two-dimensional particle-in-cell (PIC) simulation using a finite-difference time-domain method is used to study HPM multipactor and plasma avalanche in an ambient local high pressure above a dielectric window. A plane electromagnetic wave propagated in a double-parallel-plate transmission line is normal incident to the dielectric. Vaughan's secondary emission Model is used to calculate the secondary emission yield (SEY). The parameters used in simulation are: peak SEY for normal incidence δ_m=2.15, the electron energy at the peak ε_m=400 eV, the surface roughness k_s=1, the frequency f =9.3 GHz, the peak electric field E_{rf0}=40 kV/cm, N_2 gas with a pressure of 0.75Torr, and ionization only occurs in an area with a thickness of 5mm above the dielectric surface.

Define the electrons colliding the dielectric surface to generate the secondary electrons are multipactor electrons, which can ionize the gases in the ambient high pressure layer. It is illustrated in Fig.5 that the plasma discharge in the ambient desorbed gases above the dielectric surface has a thickness of several millimeter (Red curve). The plasma has a lower density at the dielectric surface due to the diffusion loss, while the secondary electron multipactor occurs on the dielectric surface, charging the surface, desorbing gases and ionizing the gases. Since the density of multipactor electrons is higher than that in plasma near the dielectric surface, a higher density ion layer above the dielectric is formed compared to other area. The density difference between the electrons and ions in conjunction with the surface charge forms a space charge field normal to the dielectric surface. It should be emphasized that the definition of multipactor electrons, different from that in Ref. [9], is more reasonable since the higher-energy multipactor electrons definitely can cause ionization avalanche, increasing the ion density above the dielectric and leading to a higher space charge field, which has an important effect on the post-pulse ionization. After the microwave pulse, plasma develops to a higher density but a narrowed width (Black curve), and this density further increases and width shrinks towards the dielectric surface (Blue curve). The diffusion loss rather than recombination loss leads to the plasma density decreasing at other place. The gas diffusion accompanying the local pressure decrease, and gases in the new diffused area could not be effectively ionized without HPM, and the residual ionization happens in the space charge sheath, where the electrons are accelerated to relatively high energy.

This project was supported by NSFC:11105108.

REFERENCES

[1] J. Benford, J. A. Swegle, and E. Schamiloglu, High Power Microwaves, Taylor and Francis, New York, 2007.
[2] Y. Y. Lau, J. Verboncoeur, and H. Kim, Appl. Phys. Lett. 89, 261501 (2006).
[3] A. Neuber, H. Krompholz, L. Hatfield, and M. Kristiansen, IEEE Trans. Plasma Sci. 28, 1593 (2000).
[4] C. Chang, et al., J. Appl. Phys., 105, 123305, 2009.
[5] C. Chang, et al., Phys. Plasmas, 16, 083501, 2009.
[6] C. Chang, et al., Appl. Phys. Lett., 96, 111502, 2010.
[7] C. Chang, et al., Appl. Phys. Lett., 97, 141501, 2010.
[8] C. Chang, et al., Phys. Plasmas 18,055702 (2011).
[9] H. Kim and J. Verboncoeur, Phys. Plasmas 12,123504 (2005).